Environmental Science & Technology

Article

pubs.acs.org/est

Novel Active Personal Nanoparticle Sampler for the Exposure Assessment of Nanoparticles in Workplaces

Chuen-Jinn Tsai,*[,†] Chun-Nan Liu,[†] Shao-Ming Hung,[†] Sheng-Chieh Chen,[†] Shi-Nian Uang,[‡] Yung-Sung Cheng,[§] and Yue Zhou[§]

[†]Institute of Environmental Engineering, National Chiao Tung University (NCTU), Hsinchu, 1001 University Road, 30010, Taiwan

[‡]Institute of Occupational Safety and Health (IOSH), Council of Labor Affairs, Executive Yuan, 99, Lane 407, Hengke Road, Shijr, Taipei, 22143, Taiwan

[§]Lovelace Respiratory Research Institute, 2425 Ridgecrest, Albuquerque 87108, United States

Supporting Information

ABSTRACT: A novel active personal nanoparticle sampler (PENS), which enables the collection of both respirable particulate mass (RPM) and nanoparticles (NPs) simultaneously, was developed to meet the critical demand for personal sampling of engineered nanomaterials (ENMs) in workplaces. The PENS consists of a respirable cyclone and a micro-orifice impactor with the cutoff aerodynamic diameter (d_{pa50}) of 4 μm and 100 nm, respectively. The micro-orifice impactor has a fixed micro-orifice plate (137 nozzles of 55 μm in the inner diameter) and a rotating, silicone oil-coated Teflon filter substrate at 1 rpm to achieve a uniform particle deposition and avoid solid particle bounce. A final filter is used after the impactor to collect the NPs. Calibration results show that the d_{pa50} of the respirable cyclone and the micro-orifice impactor are 3.92 ± 0.22 μm and 101.4 ± 0.1 nm, respectively. The d_{pa50} at the loaded micro-Al_2O_3 mass of 0.36−3.18 mg is shifted to 102.9−101.2 nm, respectively, while it is shifted to 98.9−97.8 nm at the loaded nano-TiO_2 mass of 0.92−1.78 mg, respectively. That is, the shift of d_{pa50} due to solid particle loading is small if the PENS is not overloaded.

Both NPs and RPM concentrations were found to agree well with those of the IOSH respirable cyclone and MOUDI. By using the present PENS, the collected samples can be further analyzed for chemical species concentrations besides gravimetric analysis to determine the actual exposure concentrations of ENMs in both RPM and NPs fractions in workplaces, which are often influenced by the background or incident pollution sources.

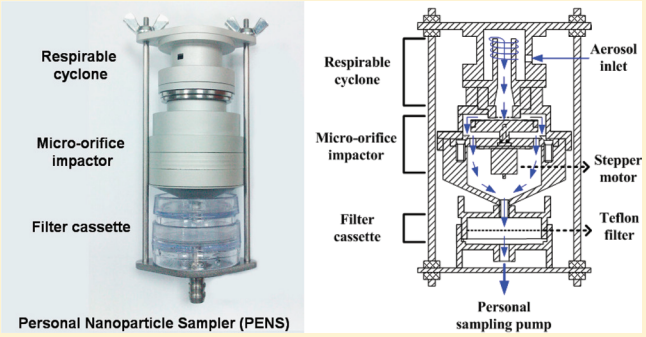

INTRODUCTION

The development and commercialization of nanotechnology have been growing very rapidly over the past few decades. As more engineered nanomaterials (ENMs) are being incorporated into products or devices, concerns about potential environmental and occupational health implications also increase. In particular, workers in the nanotechnology-based industry deserve more attention as they may have the greatest risk to expose to ENMs that lead to adverse health effects.[1−3] Furthermore, many toxicological and epidemiological studies have shown that inhaled ENMs pose a higher adverse effect than that of large particles, because the number and surface area concentrations of ENMs are much higher than those of large particles with the same mass.[1] Therefore, the assessment of the potential occupational health risks due to the exposure to ENMs is essential to ensure their safe manufacturing and handling in the workplaces.

Personal sampling is a better way to ensure accurate representation of the worker's exposure to ENMs than sampling at a fixed location.[1] However, commercial samplers that sample particles in the nanosized range such as the micro-orifice uniform deposit impactor (MOUDI),[4] the low pressure impactor (LPI),[5] or the electrical low pressure impactor (ELPI),[6] and so forth are too heavy to be used as a personal sampler. The Marple personal cascade impactor was developed as a personal cascade impactor with the d_{pa50} of 21 to 0.4 μm in its 0−8 stages and an after filter, which does not cover the nanosized range.[7] Therefore, many studies have been devoted to the development of a personal nanoparticle sampler. For example, a thermal precipitator (TP) was designed as a personal sampler to deposit nanoparticles uniformly on a colder plate by a uniform temperature gradient.[8,9] The morphology, crystallography, and chemical composition of the deposited particles could be further analyzed by using scanning electron microscopy (SEM) or transmission electron microscopy

Received: December 20, 2011
Revised: March 5, 2012
Accepted: March 21, 2012
Published: March 21, 2012

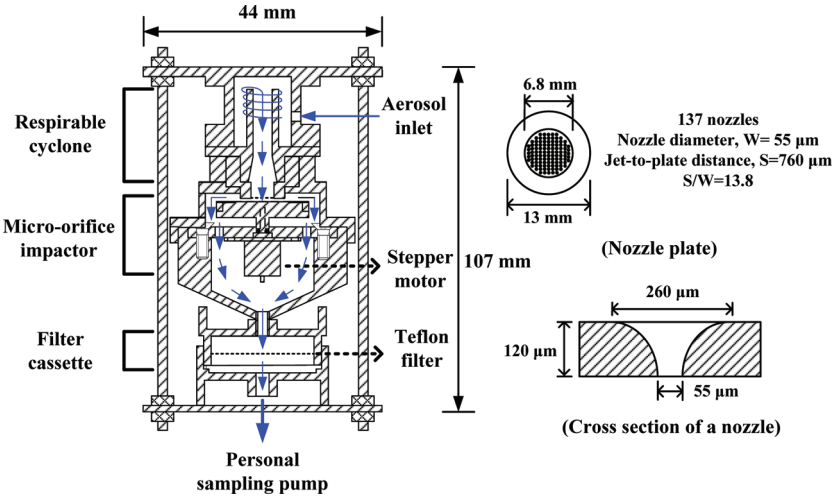

Figure 1. Schematic diagram of the PENS.

(TEM). The quantitative number concentrations can be estimated from the particles deposited on the TEM grids with the use of a model established by Lorenzo et al.[10] Miller et al.[11] developed a hand-held electrostatic precipitator to deposit nanoparticles on the substrate with collection efficiencies from 76% to 94% for nanoparticles ranging from 30 to 400 nm in diameter. However, the sampling time is too long, and the image analysis is time-consuming for these devices. In addition, particle mass collected is not adequate for subsequent gravimetric or chemical analyses. Furuuchi et al.[12] developed an active portable sampler that is able to collect a sufficient amount of NPs. Two inertial filters were assembled in series as the particle separators, and a backup filter was used to collect NPs. Nevertheless, the smallest cutoff diameter at the maximum allowable pressure drop of 5.7 kpa at 6 L/min is 140 nm only. The improvement to decrease the cutoff diameter to 100 nm or smaller is still in progress.[12] Recently, a personal respiratory dose (NRD) sampler was developed to collect particles smaller than 300 nm with an efficiency that matches with the particle deposition curve in the respiratory tract.[13]

NPs can be generated from the handling process of ENMs, high temperature combustion or reaction processes or incidental sources.[14,15] In additional to NPs, the RPM should be taken into account for the assessment of ENMs exposure in workplaces, since a large fraction of ENMs was found in the RPM due to the agglomeration of NPs or attachment of NPs to other coarse particles.[13] For representative assessment of personal ENMs exposure, therefore, it is critical to collect both NPs and respirable particulate mass (RPM) simultaneously. Many samplers have been developed for RPM sampling in the past,[16−18] in which cyclones are most widely used because their penetration curves are less sharp than those of impactors and can match with the respirable sampling criterion.[19,20] In addition, cyclones have the advantages of minimal particle bounce and re-entrainment and a high particle mass loading.[21]

In this study, a novel personal nanoparticle sampler (PENS) was designed for simultaneous active sampling of RPM and NPs by using a respirable cyclone and a micro-orifice impactor in series. Both liquid and solid particles were used to evaluate the cutoff characteristic of the PENS. The influence of solid particle loading in the PENS on the separation performance was also examined. For assessing the sampling accuracy, the measured RPM and NPs concentrations by the PENS were compared with those of a collocated MOUDI (model 110, MSP Corp. MN, USA) and a conventional respirable IOSH cyclone[20,22] in the laboratory.

Design of the PENS. As shown in Figure 1, the present sampler consists of three main parts. The first part is a respirable cyclone, which is used to classify particles larger than 4 μm in aerodynamic diameter (d_{pa}). The second part is a micro-orifice impactor with the cut-point of 100 nm. Particles ranging from 100 nm to 4 μm will impact on the impaction plate while NPs are collected by the final part, which is a filter cassette containing a 37 mm Teflon filter (Teflo R2PL037, Pall Corp., NY, USA). The size and weight of the PENS are 107 mm (length) × 44 mm (width) and 240 g, respectively. The sampling flow rate is kept at 2 L/min to ensure the pressure drop of the PENS, 14.1 kpa (respirable cyclone: 0.1 kpa, micro-orifice impactor: 13 kpa, Teflon filter: 1 kpa), is within the maximum allowable pressure drop of 21 kpa for the personal sampling pump (AirChek XR5000, SKC Inc., Eighty Four, PA, USA) used in the study. The XR-5000 pump is able to drive the PENS for more than 12 h, which is long enough for the 8 h duration of a typical work shift. More details of the pressure drop versus flow rate characteristics of the PENS and the performance curve of the personal pump can be seen in the Supporting Information (Figure S1).

The design of the present respirable cyclone is different from that of the conventional tangential flow RPM cyclone in Tsai et al.[18,20] Instead of upward direction, the air flow from the vortex finder of the cyclone exits downward directly into the micro-orifice impactor to facilitate the compact assembly of the PENS. The respirable cyclone was designed based on the dimensionless parameter, $(Stk_{50})^{1/2}$, the square root of the cutoff Stokes number, which is defined as the following:[23]

$$\sqrt{Stk_{50}} = \sqrt{\frac{C_c \rho_p d_{pa50}^2 U_i}{9\mu D}} \quad (1)$$

where C_c is the slip correction factor, ρ_p is the particle density (kg/m^3), d_{pa50} is the cutoff aerodynamic diameter (m), U_i is the gas velocity at the inlet (m/s), μ is the air dynamic viscosity (kg/m-s), and D is the inner diameter of the cyclone (m). The design of the resiprable cyclone was similar to the IOSH 18 mm respirable cyclone developed by Tsai et al.[18,20] except that the flow direction from the vortex finder was different. For d_{pa50} = 4 μm, the side length of the tangential square inlet opening was calculated to

dx.doi.org/10.1021/es204580f | Environ. Sci. Technol. 2012, 46, 4546−4552

be 2.4 mm at the sampling flow rate of 2 L/min based on eq 1. Later, the laboratory calibration showed that the d_{pa50} was 4.7 μm. The inlet dimension was then reduced to 2.1 mm to achieve the d_{pa50} close to 4.0 μm. Details are described in the Results and Discussion section and Figure S3 in the Supporting Information.

The d_{pa50} of the micro-orifice impactor was designed to be 100 nm. The design was also based on eq 1 in which D and U_i were replaced by the nozzle diameter and air speed at the nozzle, respectively. Referring to $(Stk_{50})^{1/2}$ of the ninth stage of the MOUDI,[4] which is 0.62, the micro-orifice plate was designed to have 137 nozzles, each of which is 55 μm in the inner diameter. The nozzle plate with the effective diameter of 6.8 mm for the nozzles was manufactured by a semiconductor process to have a smooth nozzle shape, as shown in Figure 1. To achieve a uniform particle deposition and avoid solid particle bounce, a stepper motor (SPC-15RF, Epoch Electronics Corp., Japan) powered by eight AA nickel−metal hydride (Ni−MH) rechargeable batteries was used to rotate the impaction plate at 1 rpm while the nozzle plate was fixed.

EXPERIMENTAL SECTION

The experimental procedure is described briefly in this section. More details can be seen in the Supporting Information (Figure S2). The inner wall loss of nanoparticles in the PENS without the micro-orifice impactor in place was first determined by using monodisperse liquid oleic acid (OA) particles classified by the TSI 3085 nano-differential mobility analyzer (DMA) with d_{pa} from 16 to 185 nm. After that, polydisperse solid microsized Al_2O_3 (or micro-Al_2O_3) particles (QF-Al-8000, Sipernat, Japan) generated by the small scale powder disperser (SSPD, TSI, model 3433) were used to calibrate the respirable cyclone, while monodispese liquid OA and solid NaCl particles classified by the TSI 3085 nano-DMA or long-DMA with d_{pa} from 16 to 560 nm and solid micro-Al_2O_3 with d_{pa} from 500 nm to 4 μm generated by the SSPD were used to calibrate the micro-orifice impactor. Solid particle loading effect on the collection efficiency of the micro-orifice impactor was conducted, and the shift of the cutoff diameter and the maximum solid particle loading capacity were also determined. The tests were conducted with nano-TiO_2 (AERODISP P25, Degussa, Germany) and micro-Al_2O_3 for the micro-orifice impactor. The following equation was used to calculate the wall loss (L) or the particle collection efficiency (η) of the respirable cyclone or the micro-orifice impactor:

$$L \text{ or } \eta = \left(1 - \frac{N_2}{N_1}\right) \times 100\% \quad (2)$$

where N_1 and N_2 are the particle concentration at the inlet and outlet of the respirable cyclone or the micro-orifice impactor measured by the TSI 3786 ultrafine condensation particle counter (UCPC) for submicrometer particles or the TSI 3310A aerodynamic particle sizer (APS) for microsized partidcles, respectively. The sharpness (σ) of the collection efficiency curves is described as the following:[17]

$$\sigma = \sqrt{\frac{d_{pa84}}{d_{pa16}}} \quad (3)$$

where d_{pa84} and d_{pa16} are the particle diameters corresponding to the collection efficiency of 84% and 16%, respectively.

After solid particle loading tests, the PENS was then used to sample the liquid OA or solid Al_2O_3 particles with the collocated MOUDI and the IOSH cyclone in laboratory comparison tests.

RESULTS AND DISCUSSION

Calibration of Particle Collection Efficiency Curves. The wall loss in the PENS for particles from 16 to 185 nm in d_{pa} without the micro-orifice impactor in place or with the cyclone only is shown in Figure 2. It is seen that the particle

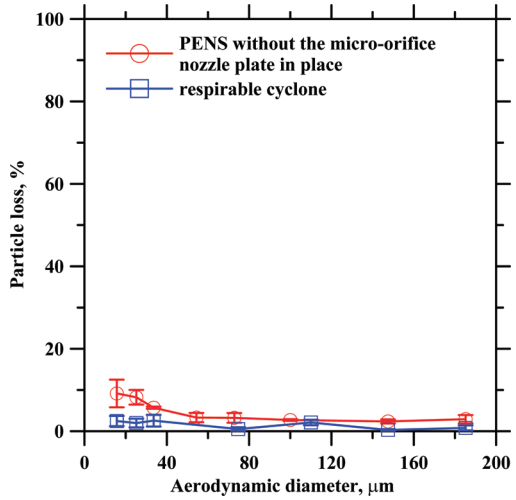

Figure 2. Liquid particle loss in the PENS without the micro-orifice impactor in place or with the cyclone only.

loss is less than 10% for the particles of all diameters, and it increases slightly with decreasing particle size due to Brownian diffusional deposition. The maximum loss occurs at d_{pa} of 16 nm, which is 9.2% for the PENS without the impactor in place or 2.5% for the PENS with the cyclone only.

The calibration results of the respirable cyclone are shown in the Supporting Information (Figure S4), which shows that the d_{pa50} of the respirable cyclone is 3.92 ± 0.22 μm and the collection efficiency for particle below 1 μm less than 5% when the side length of the square inlet is 2.1 mm. The curve matches very well with the ACGIH sampling criterion for respirable particles. In comparison, when the side length was 2.4 mm as calculated based on the design of the 18 mm IOSH cyclone, d_{pa50} was found to be 4.7 ± 0.3 μm, and the collection efficiency curve deviated very much from the sampling criterion.

Figure 3 shows the calibrated liquid particle collection efficiency curves of the micro-orifice impactor at different S/W ratios (S: jet-to-plate distance, W: nozzle diameter). This figure indicates the cutoff characteristic is very sensitive to the S/W ratio and the d_{pa50} is 82.6, 101, and 110 nm at the S/W of 9.76, 13.8, and 16.2, respectively. At S/W = 13.8, the d_{pa50} of 101 nm is very close to the desired value of 100 nm, and the collection efficiency curve is as sharp as the ninth stage of MOUDI except for particles with d_{pa} less than 90 nm. The collection efficiency has a minimum value of 5% at 60 nm below which it increases with decreasing d_{pa} with a maximum of 13.7% at 16 nm, which is due to the Brownian diffusional deposition mentioned previously. The reason why the collection efficiency is slightly less sharp when d_{pa} is less than 90 nm is because of the low nozzle Reynolds number of 385 used in the present micro-orifice impactor, which falls outside of the desirable range of 500−3000 for achieving a sharpest efficiency curve.[24]

Figure 4 shows the solid NaCl particle collection efficiencies of the micro-orifice impactor with the aluminum foil impactor substrate coated with 0.4 mg of silicone oil (or 8.75 μm in thickness, KF96SP, Shin-Etsu Chemical Co. Ltd., Taiwan) and

dx.doi.org/10.1021/es204580f | Environ. Sci. Technol. 2012, 46, 4546−4552

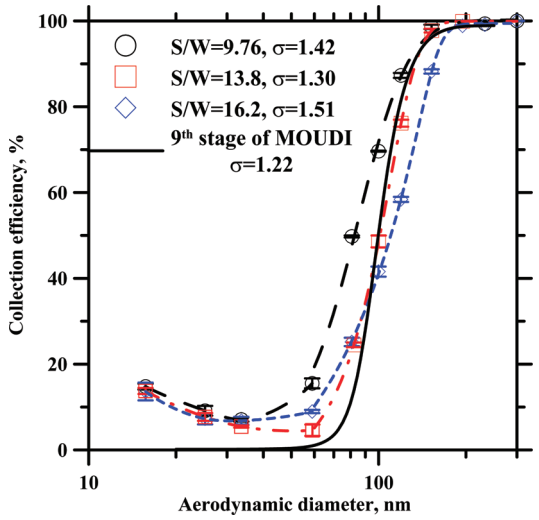

Figure 3. Liquid particle collection efficiency of the micro-orifice impactor, OA particles.

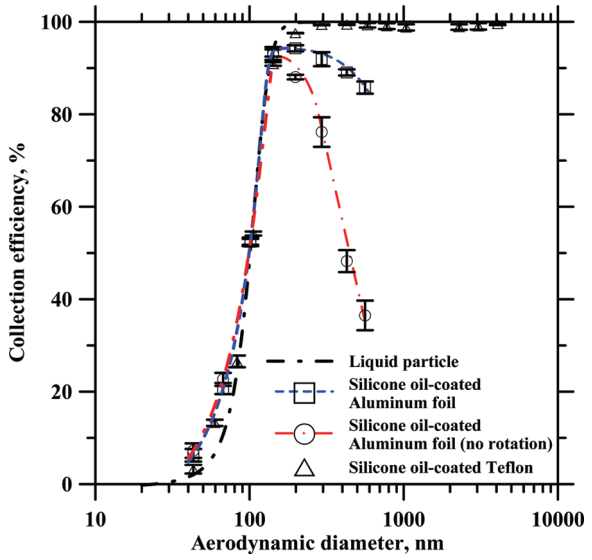

Figure 4. Solid particle collection efficiency of the micro-orifice impactor, S/W = 13.8, initially clean substrate, NaCl particles.

the substrate is initially clean. The S/W was set at 13.8. The oil-coated substrate was heated to 150 °C for 1.5 h to remove the volatile species. It is seen that solid particle bounce occurs when d_{pa} > 200 nm whether the substrate is rotating or not. The collection efficiency for the nonrotating impaction plate is much lower than that with the rotating impaction plate due to more severe solid particle bounce. For the rotating impaction plate, the collection efficiency reaches a maximum value of 94% at d_{pa} = 200 nm and then starts to decline to 85% at d_{pa} = 560 nm. This result is different from a previous study by Pak et al.[25] who only conducted a solid particle bounce test for the fifth or sixth stage of the MOUDI (d_{pa50} = 1 or 0.56 μm) and concluded that bounce was almost entirely eliminated by using the silicone oil-coated substrates with the coating thickness of only 0.3 μm. This difference is due to a much smaller d_{pa50} of the present micro-orifice impactor of 100 nm and much higher air jet velocity from the nozzle of 105 m/s. In comparison, the jet velocity in Pak et al.[25] is only 50 m/s. In Figure 5, the air jet is seen to disperse silicone oil on the substrate leaving an oil-free spot under each of the 137 nozzles, even when the substrate is rotating. The photograph was taken after introducing clean air through the PENS for 2 h. For the nonrotating substrate, similar oil-free spots were observed, and there was a small solid particle mound formed underneath each nozzle leading to more severe particle bounce.[26]

An oil-soaked sintered metal disk was used as the impaction substrate to reduce solid particle bounce as the pores of the metal could serve as oil reservoirs.[27] However, a sintered metal disk is too heavy and not suitable for subsequent gravimetric or chemical analyses. Turner and Hering[28] used an oil-coated Teflon membrane filter with a pore size of 10 μm and found it had the same solid particle collection characteristics as that of an oiled sintered metal disk. The good solid particle sticking efficiency was attributed to the pore structures of the Teflon membrane filter for holding the oil. Here, a 10 μm Teflon filter (PTU 1002550, Sterlitech Corp., USA) coated with silicone oil was used as the new impaction substrate supported by the aluminum foil to avoid solid particle bounce.

Figure 4 shows that, when the Teflon filter was coated with 10 mg of silicone oil, the collection efficiency curve of solid particles is very close to that of the liquid particles, with the d_{pa50} and GSD of 103 nm and 1.39, respectively. Furthermore, the collection efficiencies for a particle ranging from 500 nm to 4 μm are very close to 100%, which indicates that the oil-coated Teflon filters enable the effective capture of microsized solid particles with negligible solid particle bounce.

Solid Particle Loading Effect. The results in the previous section apply to initially clean impaction substrates only. For the substrate loaded with more solid particle mass, the influence on the cutoff characteristics was also investigated. With the silicone oil-coated Teflon filter as the rotating substrate, the collection efficiency curves of the micro-orifice impactor after loading with micro-Al_2O_3 and nano-TiO_2 are shown in Figure 6a and b, respectively. For micro-Al_2O_3 loading, the collection efficiency curves at different loaded mass from 0.36 to 3.18 mg are seen to be almost the same as those of clean substrates (Figure 6a). The d_{pa50} at the loaded masses of 0.36, 1.36, 2.35, and 3.18 mg is 102.9, 102.6, 101.5, and 101.2 nm, respectively, and the corresponding σ of the efficiency curves are 1.49, 1.41, 1.47 and 1.47, respectively. This means there is only a 1.7% shift of d_{pa50} and a negligible change of the shape of collection efficiency curves. Most of solid particles are now embedded in the oil-coated porous structure of the filter instead of forming particle mounds on the substrate, which will otherwise invoke particle bounce. The collection efficiency for particles from 200 nm to 4 μm remains very close to 100% indicating a good loading capacity of the substrate. Similarly for the nano-TiO_2 loaded substrates, solid particles do not bounce after heavy particle loading up to 3.42 mg. The d_{pa50} shifts to 98.9, 97.8, and 83.3 at the loaded mass of 0.92, 1.78, and 3.42 mg, respectively, and the corresponding σ was increased to 1.79, 1.85, and 2.24, respectively. Slightly higher collection efficiency was observed for particles smaller than 100 nm when loading with nano-TiO_2 particles because the substrate becomes rough with loaded particles that increase the collection efficiency of small particles. For loading with micro-Al_2O_3 particles, the increase is much less obvious for particles smaller than d_{pa50}.

Hence, the PENS can handle at least 1.78 or 3.18 mg of nano- or microsized particle loaded mass, respectively, with a less than 5% shift to a smaller value for d_{pa50}, and a negligible solid particle bounce. In other words, the limitation for operating the PENS in a typical 8 h work shift sampling is that the

dx.doi.org/10.1021/es204580f | Environ. Sci. Technol. 2012, 46, 4546–4552

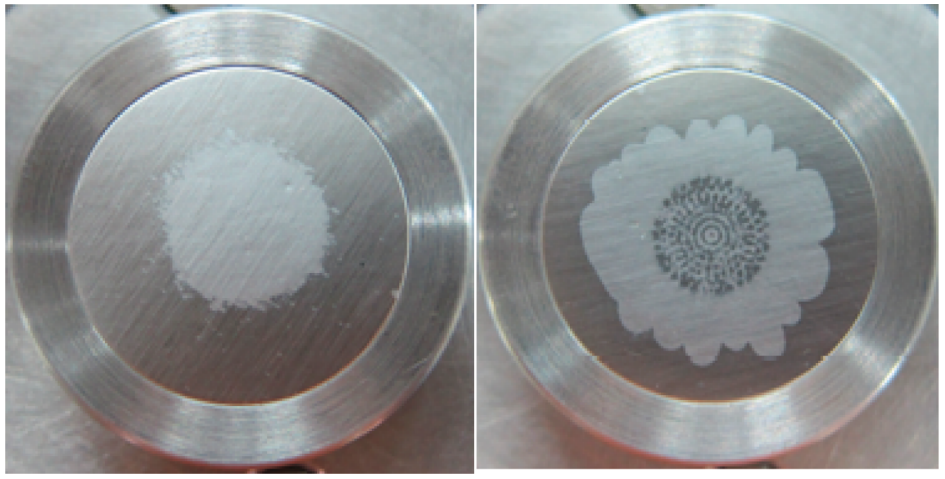

Figure 5. Photographs of the silicone oil-coated aluminum foil before and after introducing clean air through the PENS for 2 h.

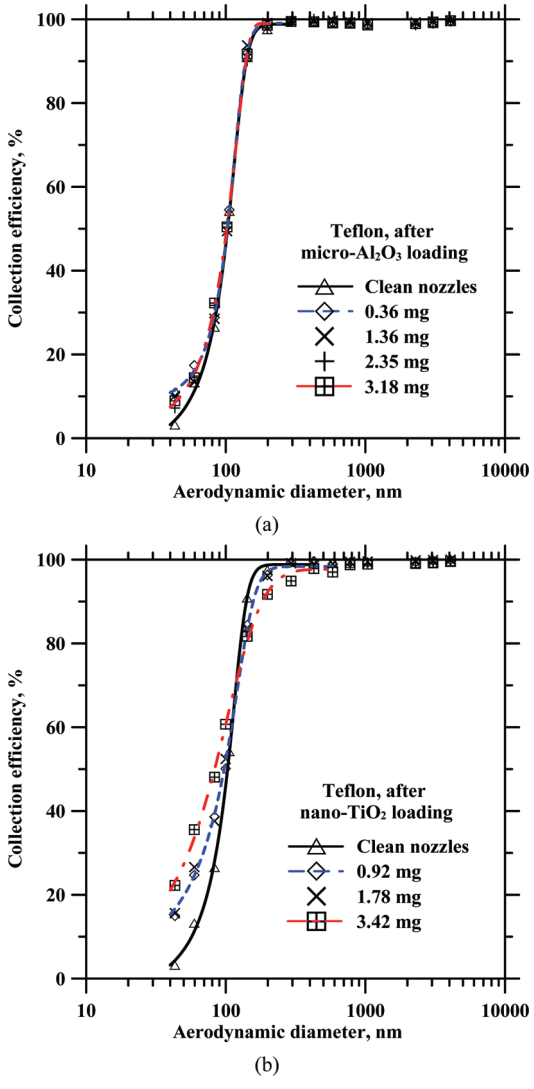

Figure 6. Particle collection efficiency curves of the micro-orifice impactor after loading with different masses of (a) micro-Al_2O_3 and (b) nano-TiO_2 particles.

average concentration must be lower than 1.85 or 3.3 mg/m^3, respectively, for NPs and RPM in the workplaces.

Effect of *S/W* on Cutoff Characteristic of the Micro-orifice Impactor. As discussed previously, *S/W* has an effect on the cutoff characteristic of the micro-orifice impactor, and such effect was studied further at several *S/W* ratios from 3.13 to 16.2. Results are shown in Figure 7, where $(Stk_{50})^{1/2}$ is

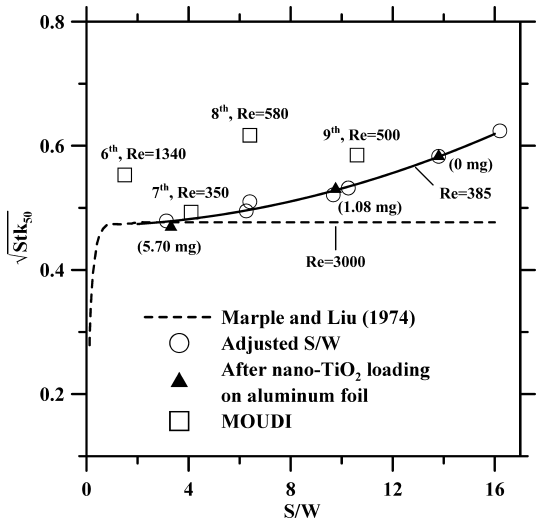

Figure 7. Relationship between $(Stk_{50})^{1/2}$ and *S/W* value of the micro-orifice impactor.

plotted against the *S/W* ratio. For the present micro-orifice impctor, $(Stk_{50})^{1/2}$ is increased gradually from 0.479 to 0.624 with the increasing *S/W* from 3.13 to 16.2. These results are different from the previous finding based on the single nozzle impactor,[29] where $(Stk_{50})^{1/2}$ was found to reach to a constant value of 0.49 when the *S/W* ratio is greater than 1. This difference is perhaps due to the radial cross-flow effect for the impactor with multiple nozzles such that the nozzles at difference radial positions may have different particle collection efficiencies. Further study of this effect is currently in progress.

The data points obtained from the nano-TiO_2 particles loaded on the silicone oil-coated aluminum foil substrate with 0–5.7 mg loaded mass also follow the same trend. The jet-to-plate distance is reduced from 760 μm (or *S/W* = 13.8) when the substrate is initially clean (or 0 mg of loaded mass) to 540 μm (or *S/W* = 9.8)

dx.doi.org/10.1021/es204580f | Environ. Sci. Technol. 2012, 46, 4546–4552

and 180 μm (or S/W = 3.3) when the loaded particle mass on the substrate is increased to 1.08 mg and 5.7 mg, respectively, which reflects in the reduction of $(Stk_{50})^{1/2}$ and the shift of d_{pa50} from 100 nm to 88.6 and 69.4 nm, respectively. In contrast, when the silicone oil-coated Teflon filter is used, no obvious solid particles accumulated on the substrate surface was observed for loaded mass up to 3.18 mg as most particles were embedded inside the pores of the filter. Therefore, a very minimum shift of the d_{pa50} and the efficiency curve are observed as shown in Figure 6. This is the additional advantage of using the oil-coated Teflon filter as the impaction substrate.

Laboratory Comparison Tests. Figure 8a and b shows the comparison of the NPs and RPM concentrations, respectively,

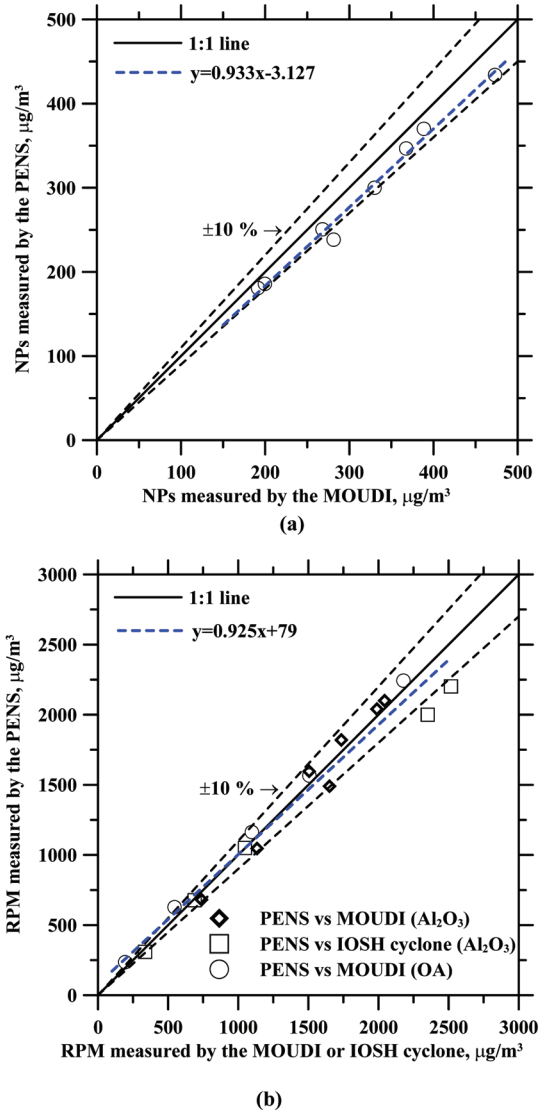

Figure 8. Comparison of the concentrations measured by the PENS and those by the MOUDI and IOSH respirable cyclone for (a) NPs and (b) RPM.

sampled by the PENS with those of the collocated MOUDI (flow rate: 30 L/min) and the IOSH resiprable cyclone (flow rate: 2.15 L/min). For NPs comparison, the tests were conducted using liquid OA particles (NMD = 100−200 nm), and only the ninth stage impactor (d_{pa50} = 100 nm) was used in order to avoid NPs loss in the upper stages. Results show that the NP concentrations measured by the PENS are very close to those of the MOUDI with a correlation coefficient (R^2) of 0.988. Slightly higher NP concentrations measured by the PENS than those of the ninth stage of the MOUDI are due to the fact that the collection efficiency curve of the micro-orifice impactor is less sharp for particles smaller than 90 nm. This means more particles with d_{pa} less than 90 nm will penetrate the micro-orifice impactor leading to a slightly higher NPs concentration. For the comparison of RPM concentrations, the tests were conducted using liquid OA and micro-Al_2O_3 particles (NMAD = 1 μm). The MOUDI with the 10th stage impactor (d_{pa50} = 56 nm) removed and the IOSH respirable cyclone were used for the comparison. For the MOUDI, the respirable mass of each stage was calculated according to the ACGIH criterion, and the RPM was calculated as the sum of the respirable mass at all stages. Results show that the RPM concentrations measured by the PENS agree well with those of the MOUDI and IOSH cyclone with the R^2 of 0.966.

The above results show that the current PENS is able to sample solid or liquid RPM and NPs simultaneously with good accuracy. Compared to the existing personal nanoparticles sampler,[7,12,13] the PENS has the lowest cutsize of 100 nm with a reasonably low pressure drop and is operable by a personal sampling pump. Currently, the personal sampling data of both RPM and NPs are largely lacking for addressing the potential health risks of inhaled nanoparticles. The data collected by the PENS are expected to be able to fill this gap. However, there are some limitations when operating the PENS. First, in order to prevent the PENS from overloading and the shift in d_{pa50}, it is recommended that the average mass concentration be less than 1.85 or 3.3 mg/m^3, respectively, for the NPs or RPM for the typical 8 h sampling duration. Second, the lowest NPs concentration of the PENS must be greater than 2 μg/m^3 to ensure that the NP filters can be weighed accurately after 8 h sampling. Since in many cases nanomaterials are present as agglomerates with a diameter larger than 100 nm, sufficient amount of RPM will be collected on the substrate of the micro-orifice impactor for accurate gravimetric analysis.

■ ASSOCIATED CONTENT

Supporting Information

Details concerning the pressure drop of the PENS, experimental details, and figures of the relationship of pressure drop to flow rate, experimental set up, particle size distribution, and solid particle collection efficiency. This material is available free of charge via the Internet at http://pubs.acs.org.

■ AUTHOR INFORMATION

Corresponding Author

*Phone: +886 3 573 1880; fax: +886 3 572 7835; e-mail: cjtsai@mail.nctu.edu.tw.

Notes

The authors declare no competing financial interest.

■ ACKNOWLEDGMENTS

The authors would like to express their gratitude to the financial support of the Taiwan Institute of Occupational Safety and Health (IOSH99-A323, IOSH98-A323), the U.S. National Institute of Occupational Safety and Health (R01 OH009801), and the Taiwan National Science Council (NSC-98-2211-E-009-020-MY3).

REFERENCES

(1) *Approaches to Safe Nanotechnology: Managing the Health and Safety Concerns Associated with Engineered Nanomaterials*; National Institute of Occupational Safety and Health: Atlanta, Georgia, 2009; http://www.cdc.gov/niosh/docs/2009-125/pdfs/2009-125.pdf.

(2) Schulte, P.; Geraci, C.; Zumwalde, R.; Hoover, M.; Kuempel, E. Occupational risk management of engineered nanoparticles. *J. Occup. Environ. Hyg.* **2008**, *5* (4), 239−249.

(3) Tsai, C. J.; Pui, D. Y. H. Recent advances and new challenges of occupational and environmental health of nanotechnology. *J. Nanopart. Res.* **2009**, *11* (1), 1−4.

(4) Marple, V. A.; Rubow, K. L.; Behm, S. M. A microorifice uniform deposit impactor (MOUDI): Description, calibration and use. *Aerosol Sci. Technol.* **1991**, *14* (4), 434−446.

(5) Hering, S. V.; Flagan, R. C.; Friedlander, S. K.; Collins, J. J.; Richards, L. W. Design and evaluation of new low-pressure impactor 2. *Environ. Sci. Technol.* **1979**, *13* (2), 184−188.

(6) Keskinen, J.; Pietarinen, K.; Lehtimaki, M. Electrical low pressure impactor. *J. Aerosol Sci.* **1992**, *23* (4), 353−360.

(7) Rubow, K. L.; Marple, V. A.; Olin, J. G.; McCawley, M. A. A personal cascade impactor: design, evaluation and calibration. *Am. Ind. Hyg. Assoc. J.* **1987**, *48* (6), 532−538.

(8) Azong-Wara, N.; Asbach, C.; Stahlmecke, B.; Fissan, H.; Kaminski, H.; Sabine, P.; Kuhlbusch, T. A. J. Optimisation of a thermophoretic personal sampler for nanoparticle exposure studies. *J. Nanopart. Res.* **2009**, *11* (7), 1611−1624.

(9) Thayer, D.; Koehler, K. A.; Marchese, A.; Volckens, J. A personal thermophoretic sampler for airborne nanoparticles. *Aerosol Sci. Technol.* **2011**, *45* (6), 744−750.

(10) Lorenzo, R.; Kaegi, R.; Gehrig, R.; Scherrer, L.; Grobety, B.; Burtscher, H. A thermophoretic precipitator for the representative collection of atmospheric ultrafine particles for microscopic analysis. *Aerosol Sci. Technol.* **2007**, *41* (10), 934−943.

(11) Miller, A.; Frey, G.; King, G.; Sunderman, C. A handheld electrostatic precipitator for sampling airborne particles and nanoparticles. *Aerosol Sci. Technol.* **2010**, *44* (6), 417−427.

(12) Furuuchi, M.; Choosong, T.; Hata, M.; Otani, Y.; Tekasakul, P.; Takizawa, M.; Nagura, M. Development of a personal sampler for evaluating exposure to ultrafine particles. *Aerosol Air Qual. Res.* **2010**, *10* (1), 30−37.

(13) Cena, L. G.; Anthony, R.; Peters, T. M. A personal respiratory deposition (NRD) sampler. *Environ. Sci. Technol.* **2011**, *45* (15), 6483−6490.

(14) Tsai, C. J.; Wu, C. H.; Leu, M. L.; Chen, S. C.; Huang, C. Y.; Tsai, P. J.; Ko, F. H. Dustiness test of nanopowders using a standard rotating drum with a modified sampling train. *J. Nanopart. Res.* **2009**, *13* (1), 121−131.

(15) Tsai, C. J.; Huang, C. Y.; Chen, S. C.; Ho, C. E.; Huang, C. H.; Chen, C. W.; Chang, C. P.; Tsai, S. J.; Ellenbecker, M. J. Exposure assessment of nano-sized and respirable particles at different workplaces. *J. Nanopart. Res.* **2011**, *13* (9), 4161−4172.

(16) Tsai, C. J.; Shih, T. S.; Sheu, R. N. Characteristics of lead aerosols in different work environments. *Am. Ind. Hyg. Assoc. J.* **1997**, *58* (9), 650−656.

(17) Huang, C. H.; Chang, C. S.; Chang, S. H.; Tsai, C. J.; Shih, T. S.; Tang, D. T. Use of porous foam as the substrate of an impactor for respirable aerosol sampling. *J. Aerosol Sci.* **2005**, *36* (11), 1373−1386.

(18) Tsai, C. J.; Chang, C. S.; Chen, S. C.; Chen, P.; Shih, T. S.; Pui, D. Y. H.; Karasev, V. V.; Onischuk, A. A.; Li, S. N. Laboratory and field tests of a novel three-stage personal dust sampler for sampling three dust fractions simultaneously. *Aerosol Sci. Technol.* **2008**, *42* (1), 86−95.

(19) Hinds, W. C. *Aerosol Technology: Properties, Behavior, and Measurements of Airborne Particles*, 2nd ed.; John Wiley & Sons, Inc.: New York, 1999.

(20) Tsai, C. J.; Shiau, H. G.; Lin, K. C.; Shih, T. S. Effect of deposited particle and particle charge on the penetration of small sampling cyclones. *J. Aerosol Sci.* **1999**, *30* (3), 313−323.

(21) Cohen, B. S.; Hering, S. V. *Air Sampling Instrument*, 8th ed.; American Conference of Governmental Industrial Hygienists Inc.: Cincinnati, Ohio, 1995.

(22) Tsai, C. J.; Shiau, H. G.; Shih, T. S. Field study of the accuracy of two respirable sampling cyclones. *Aerosol Sci. Technol.* **1999**, *31* (6), 463−472.

(23) Blachman, M. W.; Lippmann, M. Performance characteristics of the multicyclone aerosol sampler. *Am. Ind. Hyg. Assoc. J.* **1974**, *35*, 311−326.

(24) Marple, V. A.; Willeke, K. Impactor design. *Atmos. Environ.* **1976**, *10* (10), 891−896.

(25) Pak, S. S.; Liu, B. Y. H.; Rubow, K. L. Effect of coating thickness on particle bounce in inertial impactors. *Aerosol Sci. Technol.* **1992**, *16* (3), 141−150.

(26) Tsai, C. J.; Cheng, Y. H. Solid particle collection characteristics on impaction surfaces of different designs. *Aerosol Sci. Technol.* **1995**, *23* (1), 96−106.

(27) Reischl, P. R.; John, W. The collection efficiency of impaction surfaces. *Staub - Reinhalt. Luft* **1978**, *38*, 55.

(28) Turner, J. R.; Hering, S. V. Greased and oiled substrates as bounce-free impaction surfaces. *J. Aerosol Sci.* **1987**, *18* (2), 215−224.

(29) Marple, V. A.; Liu, B. Y. H. Characteristics of laminar jet impactors. *Environ. Sci. Technol.* **1974**, *8* (7), 648−654.